Geometry-Aware Metropolis Light Transport: Supplemental Results

HISANARI OTSU, Karlsruhe Institute of Technology and The University of Tokyo
JOHANNES HANIKA, Karlsruhe Institute of Technology
TOSHIYA HACHISUKA, The University of Tokyo
CARSTEN DACHSBACHER, Karlsruhe Institute of Technology

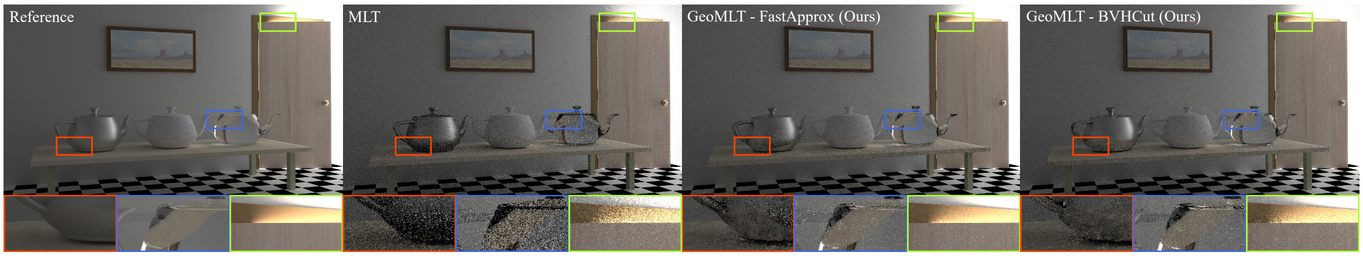

Fig. 1. Equal-time comparisons (30 minutes) of the *Ajar door* scene between MLT and GeoMLT (Ours). The images are same as teaser of the main paper, except for the image with FastApprox.

1 SUPPLEMENTAL RESULTS

Additional Image in Teaser. Fig. 1 shows rendered images of the *Ajar door* scene with MLT and GeoMLT using *FastApprox* and *BVHCut*. This figure is same as the teaser of the main paper except for the image for *FastApprox*. We can see that *BVHCut* could alleviate the discontinuity in errors due to the inaccurate approximation of the cone estimation (e.g., sides of metal teapot).

Truncation Parameters. Fig. 2 shows the error images with changing truncation parameter t_2. We parameterized the upper bound of the truncation parameter as $t_2 = (1-\varepsilon)\cdot L$ where $\varepsilon = 10^{-i}, i \in \{1,2,3,4\}$. In both cases, we can observe that error is higher in the case of $i = 1$, because the cone angle estimation with large ε tends to miss the small detail of the geometry. On the other hand, the error becomes stable as ε gets smaller. We note that *BVHCut* is more stable than FastApprox.

Structural Dependency. Fig. 3 shows the change of the rendered images of the when the scene is rotated around the up vector. The rotation happens both for the scene and the camera so the rendered images are same except for the acceleration structure. This figure corresponds to the error images in the main paper (Fig. 19). Just like the error images, we can see the discontinuity in errors (e.g., the line-shaped artifact above teapots in the image of 45 degrees) is alleviated by *BVHCut*.

Equal-Sample Comparisons. In addition to the equal-time comparisons in the main paper, Fig. 4 shows the renderings of the same four scenes (*Ajar door*, *Dining room*, *Salle de bain*, and *Staircase*) with equal-samples of 10^9 mutations. Fig. 5 shows the error distributions. The images are computed with the same machine with an Intel Xeon E7-8867 v3 at 2.5 GHz using 128 threads. These results supplements the discussion about the quality of exploration and the plot of the asymptotic error behavior in the main paper (Fig. 15). Unlike the equal-time cases, we can observe that the results with *BVHCut* outperform those of *FastApprox* in all cases. This is because the equal-sample comparisons can compensate the computational overhead of *BVHCut*.

Animation. We compared the three approaches with the animated version of the *Ajar door* scene using MLT and GeoMLT (supplemental videos). The camera position is fixed and the viewing direction is moving from left to right. All videos are rendered with 40 frames in 2 seconds (20 fps) using the same machine that we used for Fig. 4. Each frame takes 5 minutes to render. The comparisons show that the overall errors for GeoMLT are improved in the corresponding frames compared to MLT. Yet they also exhibit temporal artifacts of flickering brights points in all approaches. This is because our approaches inherit a limitation that MLT fails to handle temporal coherency, which is essentially orthogonal to our approach. This issue could be alleviated by extending the state space to the temporal domain [Li et al. 2015; Van de Woestijne et al. 2017]. Also it might be interesting future work to extend our geometry-aware mutation to time-dependent geometries.

REFERENCES

Tzu-Mao Li, Jaakko Lehtinen, Ravi Ramamoorthi, Wenzel Jakob, and Frédo Durand. 2015. Anisotropic Gaussian Mutations for Metropolis Light Transport Through Hessian-Hamiltonian Dynamics. *ACM Transactions on Graphics (Proc. SIGGRAPH Asia)* 34, 6 (2015), 209:1–209:13.

Joran Van de Woestijne, Roald Frederickx, Niels Billen, and Philip Dutré. 2017. Temporal Coherence for Metropolis Light Transport. In *Eurographics Symposium on Rendering - Experimental Ideas & Implementations.* 55–63.

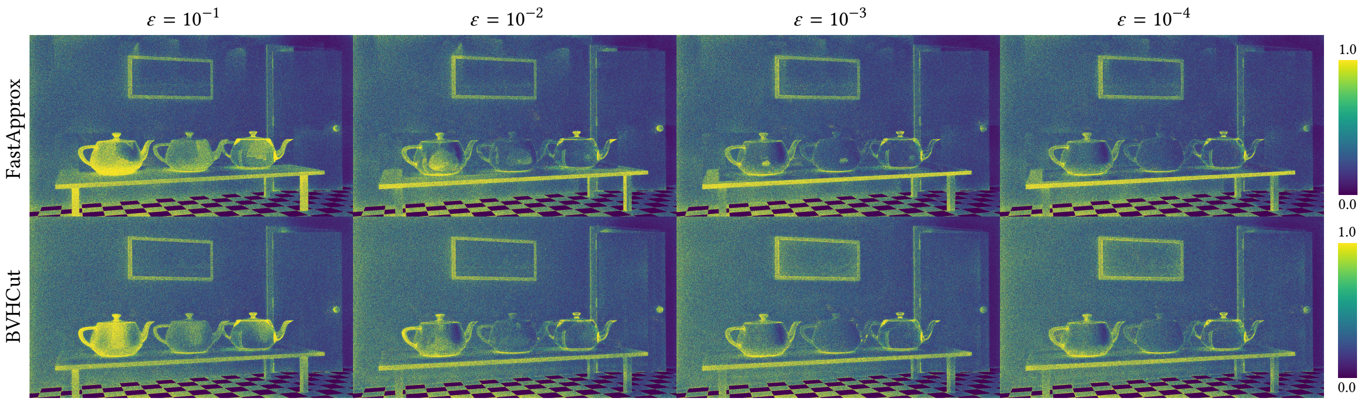

Fig. 2. Error plots (rRMSE per pixel) with different truncation parameters. BVHCut shows robust error distributions to the change of the truncation parameters compared to FastApprox , because of the subdivision of the bounds.

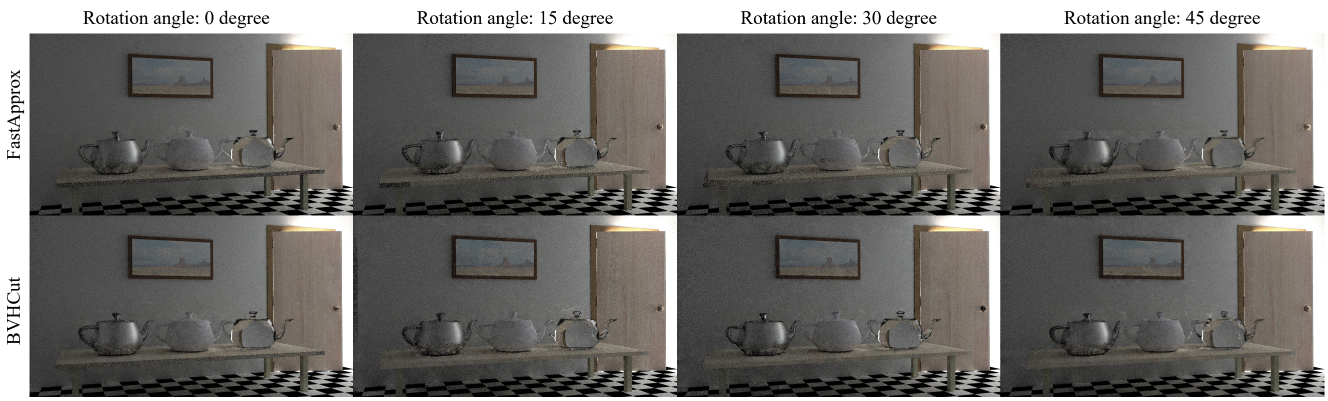

Fig. 3. Rendered images with rotated scene geometry corresponding to Fig.19 in the main paper.

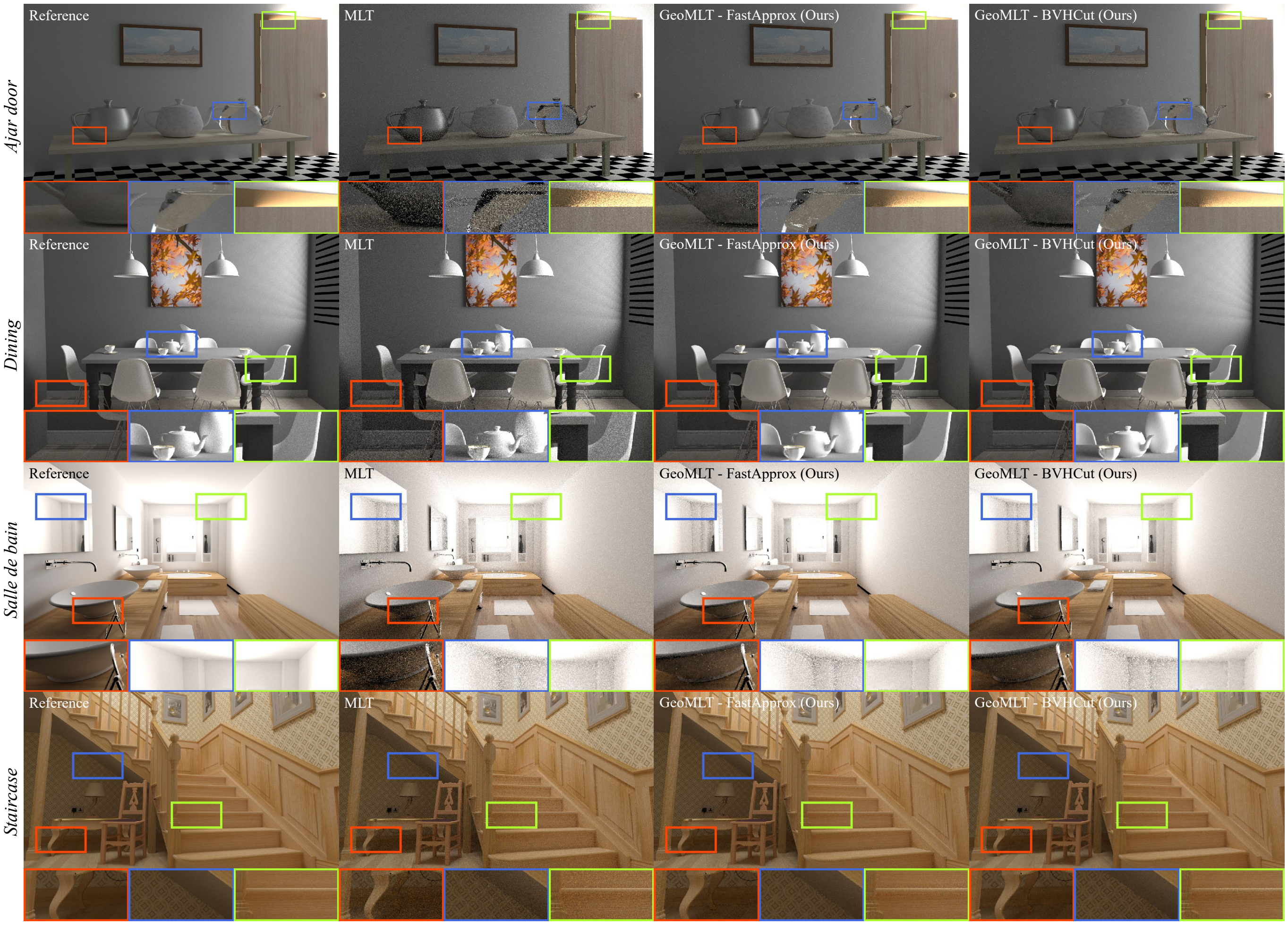

Fig. 4. Equal-sample comparisons of the scenes (*Ajar door*, *Dining room*, *Salle de bain*, *Staircase*) between MLT and GeoMLT (Ours).

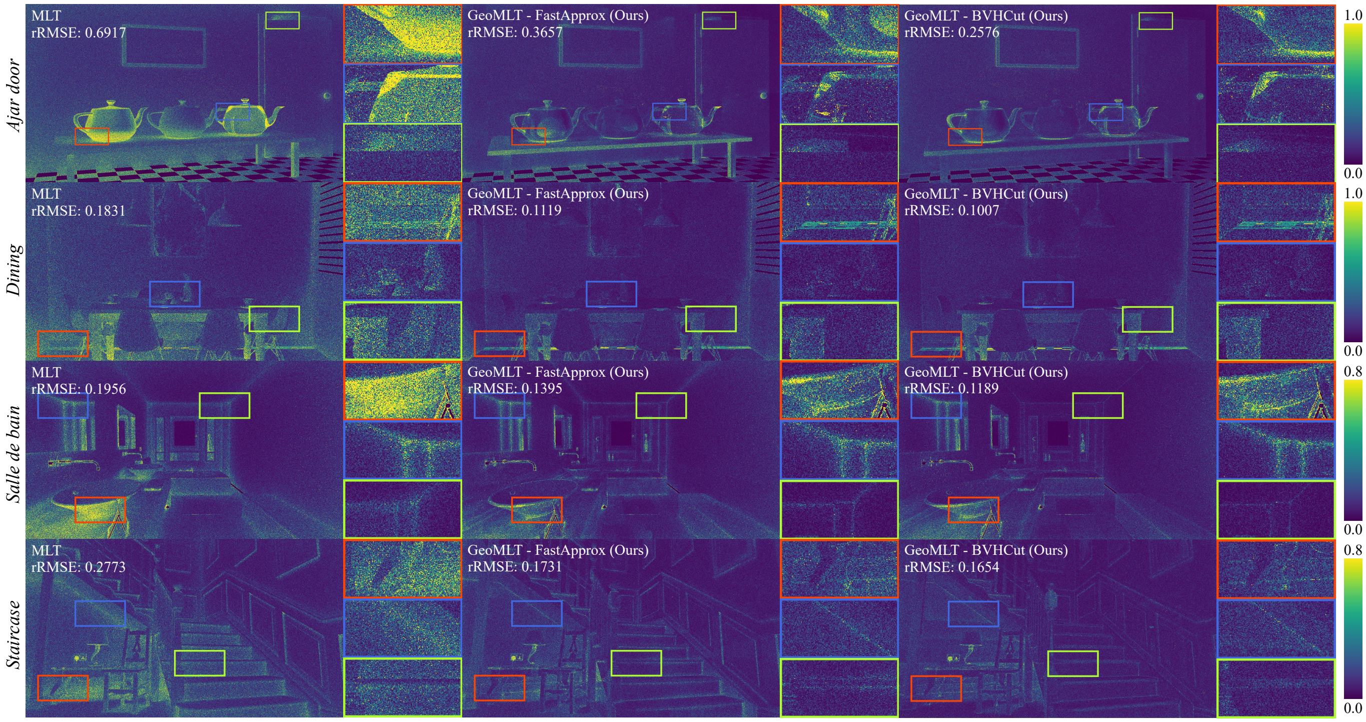

Fig. 5. Error distribution of the scenes (*Ajar door*, *Dining room*, *Salle de bain*, *Staircase*) for the equal-sample renderings in Fig. 4.